DESIGN OF CAVITY BPM PICKUP FOR EuPRAXIA@SPARC_LAB

Sh. Bilanishvili*[1], INFN LNF, Frascati, Italy

[1]also at Kutaisi International University, Kutaisi, Georgia

Abstract

EuPRAXIA@SPARC_LAB [1, 2] will make available at LNF a unique combination offering three different options. A high-brightness electron beam with 1 GeV energy generated in a novel X-band RF linac; A PW-class laser system, and a compact light-source directly driven by a plasma accelerator. Plasma and conventional RF linac driven FEL provide beam with parameters of 30- 200 pC charge range, 10-100 Hz repetition rate, and 1 GeV electron energy. The control of the charge and the trajectory monitoring at a few pC and a few µm is mandatory in this machine. Particularly in the plasma interaction region, where the pickup resolution under 1 µm is required.

As a possible solution, a cavity beam position monitor (cBPM) is proposed. A prototype in the C-band frequency range has been designed. The pickup was optimized for low charge and single-shot bunches. Here is presented the process to achieve the required specifications. The simulations were performed to study RF properties and the electromagnetic response of the device.

INTRODUCTION

While designing a cavity BPM, each dimension is chosen to improve the overall system resolution and provide a simple and efficient mechanical structure. With an increase in the resonant frequency of a cavity, the entire pick-up structure's size decreases. A cavity BPM structure designed in the C-band frequency range will be compact while large enough to be machined with sufficient accuracy [3].

The pick-up's working frequency was decided to be 5.1 GHz to reduce possible interference with the X-band Linac operating frequency 11.994 GHz. The other important specifications, that are decisive in the development process of the cBPM prototype, are loaded quality factor Q_L, the sensitivity, and required resolution that were determined according to the beam specifications for the EuPRAXIA@SPARC_LAB project, these parameters for the monitor prototype are listed in the Table 1.

Table 1: The Requried Parameters for CBPM Prototype

Parameter	Value
Frequency f	5.1 GHz
Loaded quality factor Q_L	≈500
Sensitivity	5 V/nC/mm
Resolution	<1 µm

As displayed in Fig. 1, the pickup consists of two cavities, the position, and the reference cavities. The working modes

are TM_{110} (first-order dipole mode) for the so-called position cavity and TM_{010} (monopole) for the reference cavity. When the beam passes through the pickup, it induces signals proportional to the product of charge and position offset in the position cavity, and to the charge only in the reference cavity. The beam position is then obtained by dividing the two signal amplitudes, which are available by utilizing properly designed couplers. In particular, the position cavity has four rectangular waveguides that couple to the dipole mode while suppressing the monopole mode that would otherwise limit the resolution of the electronics [4].
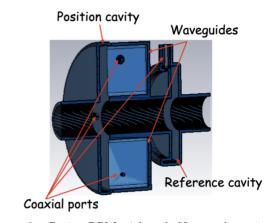

Figure 1: Cavity BPM pickup half-cut schematic view (shown: copper shell).

The waveguides are connected to the cavity volume and are placed 90° rotated to each other on one cavity sidewall. Each waveguide has a transition to a coaxial line which ends with a standard SMA connector output. In the reference cavity, the signal is coupled out through a coaxial line where the inner conductor passes through the cavity shim. The position and the reference cavities must have a sufficiently large separation distance between each other to avoid crosstalk. This distance needs to be increased with the increasing diameter of the beam pipe.

In the following sections, the pickup design with the RF characteristics of the first pickup prototype are presented.

CBPM DESIGN STUDY

The waveguide design that couple the cavity resonant modes out to the coaxial ports has a geometry that enhances the coupling between the waveguide TE_{10} mode and the cavity TM_{110} dipole mode, and rejects the coupling with the cavity monopole modes. Thus, the waveguides are a first stage filter of the common-mode coupling. Even if the common-mode coupling is ideally zero, there is always some residual coupling due to the pickup's mechanical tolerances.
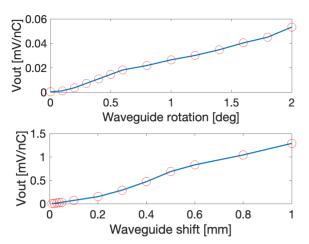
* shalva.bilanishvili@kiu.edu.ge

Figure 2: Monopole mode coupling to coaxial ports due to waveguide misaglinement errors [5].

One particular cause of residual common-mode coupling is deviations of the waveguide alignment angle and shift errors while fabrication process of the pick-up. The plots displayed in Fig. 2 show the output voltage at the cavity ports caused by the TM_{010} mode coupling, due to manufacturing errors for the mechanical position and angle of the waveguides.

Another undesired effect caused by mechanical tolerances is the coupling between the horizontal and vertical planes. Ideally, a beam crossing the cavity with a pure horizontal (vertical) offset should produce a pure horizontal (vertical) output. However, the asymmetries introduced in the geometry by mechanical tolerances cause cross-coupling between planes.
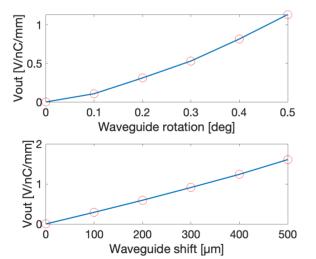

Figure 3: Dipole mode coupling to orthogonal port as a function of waveguide angle and position errors.

The main difference to the common-mode coupling is that even symmetrically perfect structure has some residual coupling between orthogonal ports, due to the quadrupole mode TM_{210}. The waveguides strongly couple this mode, but it is not possible to distinguish if the beam offset is horizontal or vertical. Due to the very low beam coupling impedance of this mode, the residual orthogonal coupling has a negligible impact on the position measurement. Figure 3 shows dipole mode cross-coupled on orthogonal port, obtained for a purely parallel beam offset, for different waveguide alignment errors.

Wakefield Simulations

After performing wakefield simulations [6], we studied the cavity's response to excitation with a charged particle bunch traveling through the beam pipe compared to the excitation on the ports used in the S-parameter simulation.

The beam simulated was a 1 mm long gaussian pulse containing 1 nC of charge. By moving the beam's position in the beam pipe, we could determine the effect of an asymmetric input on the structure.
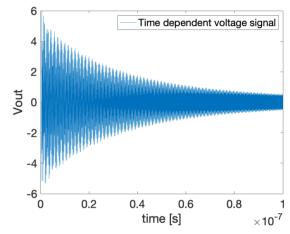

Figure 4: Raw port signal from the position cavity for 1mm offset of the beam.

Figure 4 shows the typical signal coming out of one of the ports, with a 1 mm beam offset in y. As we can see, the signal is composed by different modes, with different excitation amplitudes and decaying rates.
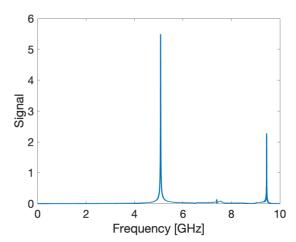

Figure 5: FFT of the position cavity port signal.

Indeed, taking the fast furier transform of the position cavity's port port signal, Fig. 5 we can see the modes that dominate at the output. The dominant mode frequency was 5.1 GHz, corresponding to the lowest order dipole mode.

When the beam is only offset in either x or y, it was the only significant signal. However, when the beam was off-axis in both dimensions, then an additional peak of the quadrupole mode, TM_{210} appeared. This response is a signature of the quadrupole mode: a beam offset in x or y only produces a symmetric field concerning the waveguides and so does not couple. However, when the beam is offset in both x and y, the symmetry gets broken, and the quadrupole mode is generated, some part of which is able to couple out into the waveguide [7].

Frequency Domain Simulations

Simulations in the frequency domain were performed [8], to evaluate the cross-coupling level between the coaxial ports. In order to do so, we registered the ends of each coaxial feedthrough as wave ports and plotted S parameters for them Fig. 6.
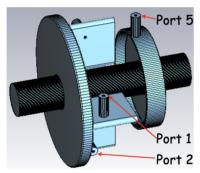

Figure 6: Cavity BPM pickup schematic view (shown: vacuum). Port 3 is on the same plane as Port 1.

As it can be seen from Fig. 7 the level of the cross-coupling between the reference and position cavities is on the level of -140 to -145 dB, which means that the distance between the resonators, 32,5 mm, provides a sufficient isolation level between them.
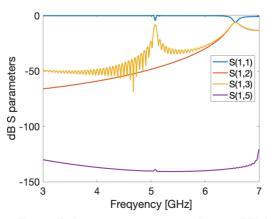

Figure 7: S-parameter response of cavity BPM.

Table 2: The Main Characteristics of CBPM Prototype

Parameter	Numerical calculation		
	TM_{010}	TM_{110}	Reference
f_{GHz}	3.419	5.100	5.100
Q_0	2800	2200	1400
Q_L	–	450	410
Damping time in ns	–	28.17	25.6
$\frac{R}{Q}$,Ohm	52	0.5	48
V_{out}	–	4.9 V/nC/mm	36 V/nC
angle/position signal ratio [deg/mm]	–	0.0163	–
Theoretical resolution	–	170 nm	–

CONCLUSIONS AND OUTLOOK

Dual-resonator cavity BPM prototype is proposed with aloaded quality factor $Q_L \approx 450$ and sensitivity S = 4.9 V/nC/mm. The approximated theoretical resolution, including only the thermal noise is ≈ 170 nm, these specifications are indcated in Table 2.

Once the first prototypes will be fabricated, bench-top measurements and beam tests will be performed. Such a new test-bench for cBPMs at SPARC_LAB at INFN-LNF was designed and will be used in the prototype's future tests.

REFERENCES

[1] M. Ferrario *et al.*, "EuPRAXIA@SPARC_LAB Design study towards a compact FEL facility at LNF", *Nucl. Instrum. Methods Phys. Res., Sect. A*, vol. 909, pp. 134-138, Nov. 2018. doi:10.1016/j.nima.2018.01.094

[2] R. W. Assmann *et. al.*, "EuPRAXIA Conceptual Design Report", *Eur. Phys. J. Spec. Top.*, vol. 229, pp. 3675–4284, 2020. doi:10.1140/epjst/e2020-000127-8

[3] A. Lunin, "High Resolution RF Cavity BPM Design for Linear Collider", In *8th DITANET Topical Workshop on Beam Position Monitors*, CERN, Switzerland, 2012.

[4] F. Marcellini *et al.*, "Design of Cavity BPM Pickups for Swiss-FEL", in *Proc. 1st Int. Beam Instrumentation Conf. (IBIC'12)*, Tsukuba, Japan, Oct. 2012, paper TUPA24, pp. 390–393.

[5] S. Bilanishvili, "Design and Studying Physical Properties of Cavity Beam Position Monitors for Electron Accelerators", Ph.D. thesis, Phys. Depart., Istituto Nazionale di Fisica Nucleare, Laboratori Nazionali di Frascati LNF, Apr. 2021.

[6] Computer Simulation Technoloty (CST), http://www.cst.com

[7] A. F. D. Morgan, S. T. Boogert, N. Y. Joshi, A. Lyapin, S. Molloy, and G. Rehm, "Simulation of a Cavity BPM for High Resolution Single-Pass Beam Position Measurements", in *Proc. 14th Beam Instrumentation Workshop (BIW'10)*, Santa Fe, NM, USA, May 2010, paper TUPSM026, pp. 168–172.

[8] ANSYS HFFS, https://www.ansys.com/products/electronics/ansys-hfss